NANO LETTERS

Letter

pubs.acs.org/NanoLett

Thermal Excitation Control over Photon Emission Rate of CdSe Nanocrystals

Benjamin T. Diroll[†] and Richard D. Schaller*[,†,‡]

[†]Center for Nanoscale Materials, Argonne National Laboratory, Lemont, Illinois 60439, United States

[‡]Department of Chemistry, Northwestern University, Evanston, Illinois 60208, United States

Supporting Information

ABSTRACT: Temperature-dependent photoluminescence lifetimes of electron−hole pairs (excitons) in CdSe nanocrystals are governed by the energetic ordering and spacing of slowly emitting, spin-forbidden "dark" exciton states and rapidly emitting "bright" states. Here, infrared pulses that are resonant with hydrocarbon surface ligand vibrational transitions are shown to offer a route to manipulate the instantaneous emission rate of CdSe nanocrystals at cryogenic temperature. Transient heating of the inorganic nanocrystal core is achieved via resonant excitation of ligand vibrations, followed by heat flow to the nanocrystal lattice. Heating of the nanocrystal core is demonstrated using transient absorption spectroscopy, which shows a time-dependent red-shift of the quantum dot electronic absorption resonances, consistent with heating. Transient heating of the nanocrystal above the bath temperature increases the instantaneous radiative rate of the nanocrystals via a combination of thermal occupation of bright states as well as phonon-assisted emission. The lifetime of this infrared-pumped, fast-emitting sample condition is dictated by particle thermalization, which is multiple orders of magnitude shorter lived than the dark exciton state. This work demonstrates the feasibility of using heat control pulses to manipulate electronic recombination rates of excitons.

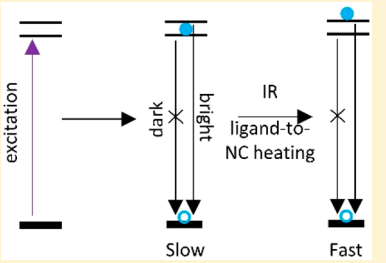

KEYWORDS: *Nanocrystal, photoluminescence, heat transfer, infrared, exciton*

Low-temperature photoluminescence (PL) of CdSe nanocrystals (NCs) has been studied extensively both theoretically and experimentally, because it offers direct insight into the electronic structure and properties of these materials.[1−9] The exciton fine structure of NCs can differ substantially from that of bulk semiconductors, resulting in size-, shape-, and crystal-polytype-dependent control over radiative lifetime and emission polarization.[4,10−15] In particular, the manifold of discretized excitonic "edge" states, which are spaced in energy by a single meV to tens of meV (depending on particle size, crystal structure, and shape), yields temperature-dependent radiative rates owing to thermally accessed occupation of states, which for sufficiently low temperatures becomes dominated by the lowest-lying exciton state. For quasi-spherical, wurtzite CdSe NCs—and, indeed, most semiconductor NCs—the lowest state is a spin-forbidden transition to the ground state and therefore termed a "dark" exciton.[1,8,13,16,17] Whereas at room temperature, the average radiative lifetime is ∼20 ns as bright excitons populate and radiate, this lifetime can dramatically increase to 1 μs at temperatures of a a few Kelvin.[8] Dynamic modulation of the occupation, energy, or radiative rate of excitonic states for a given NC has thus far been achieved with strong magnetic fields and by controlling the sample temperature.[1,8,9,18,19] The method described here permits control of the instantaneous radiative rate with a separate control pulse. In this work, by probing zinc blende CdSe NCs, temporally controlled heat excitations are shown to manipulate the radiative rate of CdSe NCs at 5 K via transient heating of the NC lattice on an ultrafast time scale.

In CdSe NCs, the exciton fine structure, which dictates low-temperature PL, depends on the size, crystal structure, and shape of NCs.[1,4,10,12,20] CdSe has eight excitonic states—0^L, 0^U, $\pm1^L$, $\pm1^U$, and ±2, in which the number refers to the angular momentum of the transition to the ground state and superscripts L and U refer to lower and upper, respectively.[12,13] In spherical and slightly prolate wurtzite systems, the lowest excitonic states are the ±2, which convey a so-called "dark" exciton because of the spin-forbidden transition to the ground state. These ±2 states are separated by 2−20 meV (depending on size) from the lowest-energy bright states, $\pm1^L$. Therefore, at sufficiently low temperatures, excitons thermalize to the dark state, and the PL lifetime increases substantially from ∼20 ns at room temperature to approximately 1 μs.[1,8] Such measurements display a fast component of emission at early time, which has been argued occurs as the phonon bath generated from intraband cooling (electron−phonon coupling) keeps the instantaneous rate of emission high until phonons are dissipated across the ligand−NC interface.[1,3,8,18,21,22] The precise reason for the higher emission rates may relate either to a greater occupation of the bright excitonic manifold or owing to changes in the radiate rate of excitonic transitions (i.e., dark

Received: December 4, 2018
Revised: March 15, 2019

DOI: 10.1021/acs.nanolett.8b04847
Nano Lett. XXXX, XXX, XXX−XXX

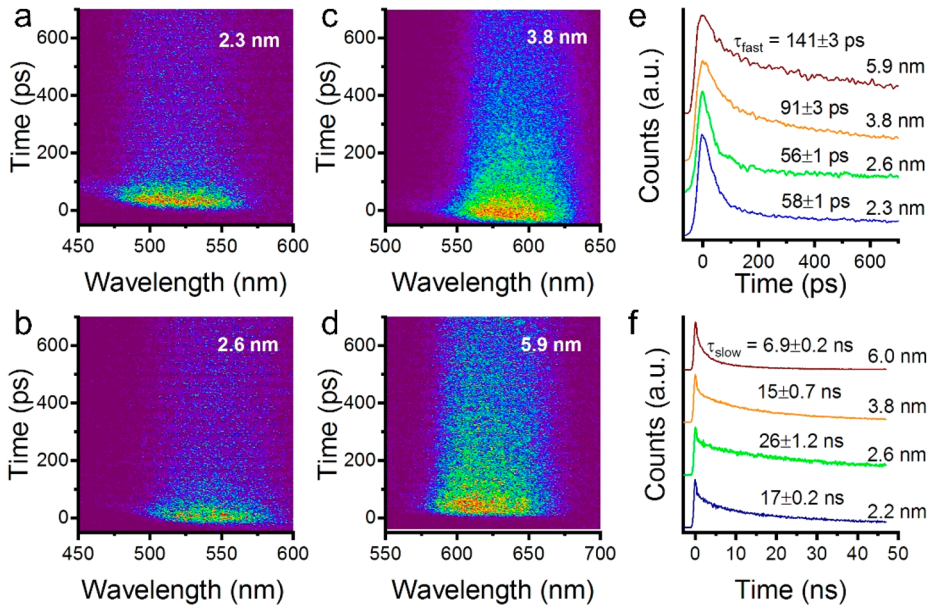

Figure 1. Time- and spectrally resolved PL of (a) 2.2, (b) 2.6, (c) 3.8, and (d) 6.0 nm zinc blende CdSe NCs collected at 5 K. (e) Time-resolved PL at early times for the series. Lifetimes are estimated from a single exponential fit to the data. (f) Time-resolved PL at longer times for the series relating exciton lifetimes. Lifetimes are estimated from a single exponential fit to the data 5 ns after the initial pulse. All data acquired with 400 nm pump.

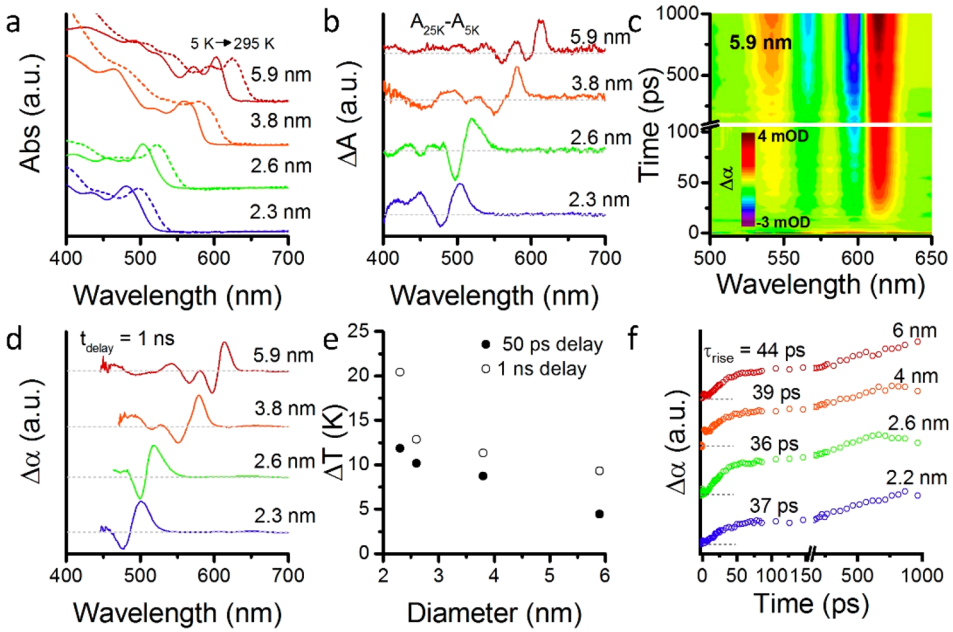

Figure 2. (a) Static absorption spectrum of zinc blende CdSe NCs taken at 5 and 295 K. (b) Differential absorption spectrum comparing the absorption of the given samples at 25 K with their absorption at 5 K. (c) Two-dimensional map of infrared pump, electronic probe (IPEP) data for 6.0 nm CdSe NCs pumped with 3460 nm light. (d) IPEP spectra for CdSe NCs at 1 ns delay time. (e) Estimated temperature rises in the NC samples at 50 ps delay from the IR pump and 1 ns delay from the IR pump. (f) IPEP kinetics for CdSe NCs at the first excitonic-feature IR-pump-induced absorption (offset for different indicated particle sizes). The fast-rise feature was fitted from the first 150 ps of data. Gray dashed lines indicate $\Delta\alpha = 0$ for each of the scans.

excitons), upon vibrational assistance of electronic recombination in the presence of phonons.

For zinc blende CdSe NCs used in this work (see X-ray diffraction in Figure S1), theoretical and experimental work is less explored but suggests that excitonic states are more closely spaced than in hexagonal systems.[12] Specifically for zinc blende CdTe, prolate NCs are expected to have ∼3 meV dark/bright splitting in 6 nm diameter particles and larger and ∼5 meV splitting in 3 nm particles.[12] The closely spaced excitonic states of zinc blende, which permit facile occupation of high-energy states, offer an advantage compared to wurtzite systems, because they are more responsive to the thermal control pulses employed as described below (vide infra). Figures 1a–d shows a sub-nanosecond decay feature for each of the zinc blende samples used in this work consistent with initial occupation of higher excitonic states of greater oscillator strength followed by

DOI: 10.1021/acs.nanolett.8b04847
Nano Lett. XXXX, XXX, XXX−XXX

a substantial slowing of photoemission (Figure 1e). These rapid decay features are followed by a much slower decay ranging from 7 to 25 ns in these samples, as shown in Figure 1f.

As noted above, the rapid decay feature observed in time-resolved PL of CdSe NCs at low temperatures reflects the thermalization of excitons within the manifold of excited states and thermal dissipation of phonon energy derived from intraband relaxation.[21] Following an excitation above the band gap, carrier cooling results from electron−phonon scattering, heating the NC lattice above the environmental temperature.[21] In addition to permitting some small change in the occupation of bright excitonic states, acoustic phonons generated as an eventual result of carrier cooling are hypothesized to reduce symmetry of the crystal structure of CdSe NCs, which transiently relaxes the spin-forbidden transition of the lowest excitonic state.[23,24] That is, both equilibrium and nonequilibrium thermal contributions may transiently increase the oscillator strength of CdSe NCs. The NC lattice itself cools via phonon−phonon coupling to the surrounding environment (i.e., coupling to organic ligand matrix and solvent, if applicable).[25−27] For wurtzite CdSe NCs, phonon−phonon coupling to the environment occurs on a tens to hundred picosecond time scale and depends chiefly on particle size, although crystal faceting and ligand coverage can change this time scale substantially in simulations.[21,22,28] Here, the fast PL decay at early time (labeled τ_{fast}) also increases somewhat for the larger NCs in this study, although the differences between the samples are much smaller than in wurtzite crystals, possibly because of the energetically smaller excitonic manifold[12] or differential coupling to the environment.[28] The slow PL decays (labeled τ_{slow}) fitted in Figure 1f, although much faster than 1 μs decays of wurtzite CdSe NCs at 5 K, are still approximately 2 orders of magnitude longer than the fast-decay feature in all samples.

The process of phonon−phonon heat outflow is reversible. Excitation of the hydrocarbon ligand C−H stretches at 3400−3600 nm (Figure S3) offer a means to generate a thermal gradient for heat flow *into* the NC.[29] Figure 2 demonstrates this phenomenon for the samples used in this work. The steady-state absorption at 5 and 295 K of the samples formed and deposited as thin films on sapphire is shown in Figure 2a. Increasing temperature of the samples results in red-shifts of the semiconductor band gap and broadening of the absorption resonances. (Photoluminescence energy as a function of temperature is recorded in Figure S4.) Figure 2b shows the difference spectrum of the static absorption (ΔA is used for static measurements; $\Delta\alpha$ is used for transient absorption data) for the four samples comparing the absorption at 25 K with the absorption at 5 K. Each of these shows an increased absorption to the red because of a heat-induced bathochromic shift of NC absorption owing to lattice expansion.

Infrared pump, electronic probe (IPEP) spectroscopy measurements of these samples employs a femtosecond pump beam here (and except where noted) centered at 3460 nm (covering ligand absorptions) followed by a white light visible probe of the semiconductor NC absorption. (See Supporting Information.) As shown in Figure 2c, a Stark effect at zero delay time[30] is followed by a rise in the $\Delta\alpha$ signal, which adopts a spectroscopic signature indicating a red-shift of the NC absorption. The IPEP spectra of the CdSe NC samples at 1 ns delay times are shown in Figure 2d, with an increase in the absorption to the red consistent with the Varshni relation and static measurements of temperature-dependent absorption of the same samples (Figure S4).[31] The similarity of the IPEP $\Delta\alpha$ spectra and the static ΔA spectra confirms that the IR excitation induces NC heating.

The temperature rise induced by the IR pump, which varied in absorbed fluence from 64 μJ/cm^2 for the 5.9 nm sample to 288 μJ/cm^2 for the 2.3 nm sample, is estimated in Figure 2e at delay times of 50 ps and 1 ns. This estimate, which ranges from 10 to 20 K at 1 ns delay time is obtained by collecting temperature-dependent measurements of the static absorption to provide a temperature calibration for the changes observed transiently. Integrations of static ΔA spectra at known temperature values are used to calibrate $\Delta\alpha$ spectra obtained from IPEP experiments. (See Figure S5 and discussion). The increasing ΔT for smaller NCs chiefly reflects a greater extinction of ligands relative to the inorganic core, because of larger surface-to-volume ratios, but may also capture effects of size-dependent heat capacity. At 5 K, such thermal excitations raise the thermal energy (kT) of the NCs by a factor of 2−5 and therefore can enable a substantial population of the excitonic states separated by <10 meV from the ground state, as is predicted for the bright states of zinc blende CdSe NCs.[12]

The dynamics of the IPEP spectra in Figure 2f display biexponential rise dynamics, with 60−70% of the signal change occurring within 150 ps. This fast component of the NC heating was fitted with a function of the form $A(1 - e^{-t/\tau_{rise}})$ to obtain characteristic heating times for the samples reported in Figure 1e. These times (τ_{rise}) vary over a small range from 36 to 44 ps, increasing slightly with the size of the NCs, qualitatively consistent with the fast-decay feature observed in the time-resolved PL data in Figure 1 and earlier work on interfacial heat flow.[21,22,29] The differences in the τ_{rise} time from IPEP measurements and τ_{fast} time from time-resolved PL measurements most likely arise from the fact that the processes are not identical reversals and possibly occur due to differences of the temperature gradient of the blue excitation versus IR excitation. Particularly noteworthy differences with IPEP measurements include the fact that heat inflow occurs *after* thermalization of high-energy vibrations into the manifold of ligand vibrational states (intramolecular vibrational relaxation or IVR),[32] and there are no contributions from carriers (or excitons), because the semiconductor NCs have not been excited.

Organic ligands serve effectively as antennae to capture thermal excitations, which are transferred to the NC core in the experimental design presented in Scheme 1. First, a blue pump excitation (400 nm) is used to generate excitons in the NC ensemble. Initially, the pump energy in excess of the band gap heats the NC through electron−phonon coupling resulting in the above-described burst of PL, followed, after subsequent lattice cooling, by slow PL decays. After a variable delay, the sample is excited with an IR pump resonant with the ligand vibrations, which heats the inorganic NC core. Thus, heated, the NCs emit a second burst of PL as the radiative rate increases for a fraction of the NC population. The design of the blue pump followed by an IR pump is in some ways analogous to earlier transient absorption measurements from Klimov et al. and Sionnest et al., although in those works, the IR source was tuned to be resonant with intraband transitions of CdSe NCs, rather than ligand vibration energies.[33,34]

Examples of this experiment for the same series of NCs in Figure 1a−d are shown in Figure 3a−d. Here, the sample

DOI: 10.1021/acs.nanolett.8b04847
Nano Lett. XXXX, XXX, XXX−XXX

Scheme 1. Simplified Schematic of Heat-Controlled Emission for NCs with Small Bright/Dark Splitting at Low Temperature[a]

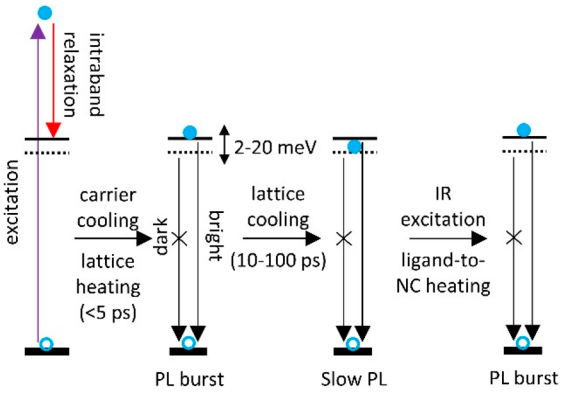

[a]Textual labeling reflects the expected behavior of an ensemble; graphics do not represent true Fermi−Dirac distributions of excitons. An alternative model suggests that phonon-assisted and -unassisted radiative rates diverge substantially. In both explanations, transient temperature elevation effects change the radiative rate.

decay induced by 400 nm pump excitation is punctuated after 500 ps by a second burst in PL as described in Scheme 1, arising because of an IR-pump beam. A comparison of the integrated dynamics with and without secondary IR pumping shown in Figure 3e, with a zoom-in in Figure 3f, shows that the secondary PL burst is particularly prominent in the smaller NC samples where the temperature rise is largest. The proportionality of the response observed in both IPEP measurements and in the IR-induced PL feature argues in favor of a common origin. Measurements with IR pumping alone confirm that multiphoton absorption does not contribute to the changes in PL with the IR pump for these samples, which have visible band gaps (Figure S6). The time-domain response of the IR-pump-induced emission is more complicated than that of interband pumping alone. The asymmetrical nature of the IR-induced features confirms that these changes are not simply due to a Stark effect.[35] The rise of the secondary PL burst occurs on a time scale consistent with that of IPEP measurements and is convolved with depletion of excitons that occupy the bright excitonic transition on a similar time scale. Except in the case of the 5.9 nm sample, the PL data without IR excitation are nearly flat, with the decay dominated by the long dark-state lifetime. Therefore, by using IPEP measurements to fix the rise time of IR-induced PL, time-resolved data with IR excitation shown with open circles in Figure 3f are fit with solid colored lines to the following convolved function

$$I(t) = A(1 - e^{-t/\tau_{rise}})(e^{-t/\tau_{IR}} + B)$$

in which the input for τ_{rise} is fixed from fitting IPEP data in Figure 2, and A and B are scalars. τ_{IR} represents the instantaneous rate of photon emission from the sample after IR excitation. Pointedly, the τ_{IR} times are consistently shorter than the τ_{fast} dynamics fit for blue pumping alone. Because both features are dictated by thermalization of carriers, this suggests that the temperature rise induced by the IR beam is somewhat smaller than the rise induced by the blue pump. The initially generated phonon population of the blue pump must first evolve to that of the smaller population of the IR pump, after which they may be expected to evolve in the same manner, leading to an elongated thermalization of the blue pump with respect to the IR pump.

Although the burst in the PL signal should in principle be seen in steady-state PL measurements with and without IR

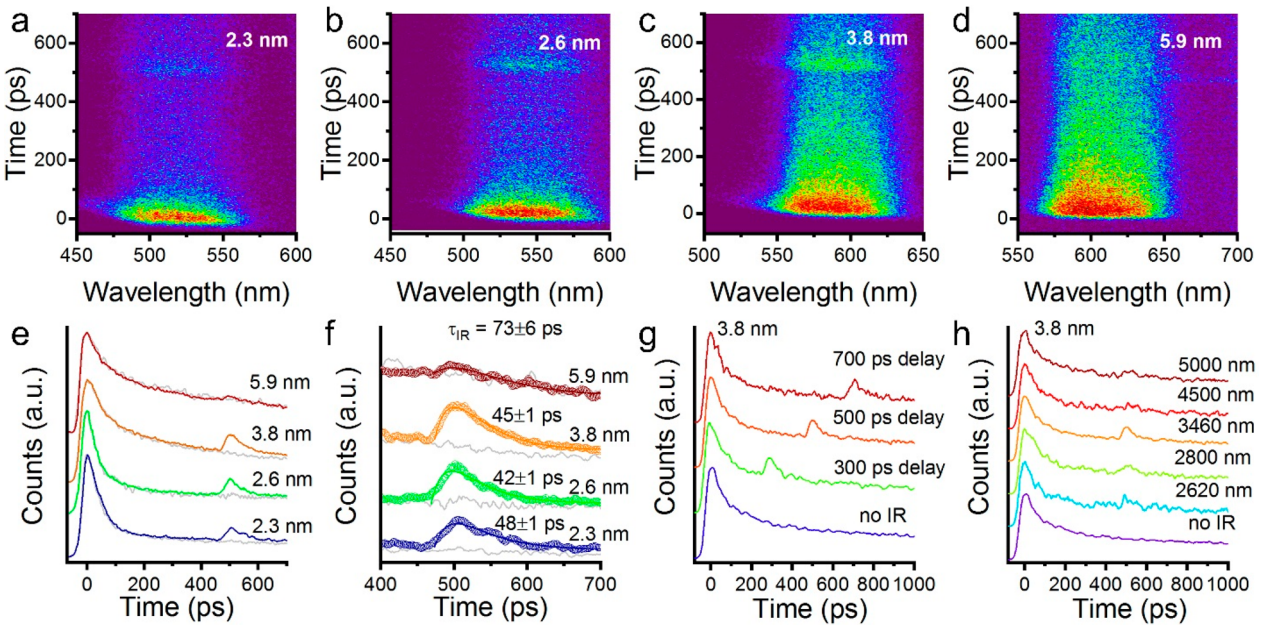

Figure 3. Time- and spectrally resolved PL of (a) 2.2, (b) 2.6, (c) 3.8, and (d) 6.0 nm zinc blende CdSe NCs collected at 5 K with initial 400 nm pump followed by 3460 nm pump for 500 ps. (e) PL dynamics of CdSe NC samples with 400 nm pump followed by 3460 nm pump in colors and gray lines representing data without IR pump. (f) PL dynamics with IR pump are shown in open circles, and data without IR pump is shown with a gray line. Solid colored lines represent a convolved fit of an exponential rise (fixed by IPEP measurements in Figure 2) and an exponential decay with time constant τ_{IR}, which are reported on the plot. (g) PL dynamics of 3.8 nm CdSe NCs excited at 400 nm followed by 3460 nm pump at different delay times. (h) PL dynamics of 3.8 nm CdSe NCs excited at 400 nm followed by 500 ps of IR pumps of different wavelengths.

DOI: 10.1021/acs.nanolett.8b04847
Nano Lett. XXXX, XXX, XXX−XXX

pumping through a change in the PL spectrum, in practice, this was not observed, because the total signal intensity arising from the PL burst is a very small fraction of the total PL under these conditions, and any effect in the time-integrated signal is masked by variations in the pump laser intensity (Figure S6). Changes in the absolute intensity of time-integrated PL are not anticipated, as there is no reason to believe that the IR pump substantially changes the quantum yield of recombination pathways. However, changes in the absolute intensity within the ~700 ps windows in Figure 3 do occur: for the 2.3, 2.6, and 3.8 nm samples, approximately 8−10% more photons are emitted in the given time window compared to the case with only interband excitation. It is important to note also that the relative strength of PL from the 400 nm excitation compared to that induced with an IR pulse is experimentally constrained by the overlap of the small IR beam with the larger blue pump beam, which limits the apparent modulation, as only a fraction of the photoexcited sample is subsequently pumped with the IR beam. (See Supporting Information for details.) This is also the reason that despite reaching higher effective temperatures with thermal excitation (at least in the smaller NCs) than with single-photon absorption and carrier thermalization, that the magnitude of PL modulation from the IR pump is smaller than that of fast component of the PL induced by the blue pump.

Additional two-pump experiments in Figure 3g show that the delay of the IR pump can be controlled precisely, here tuning from 300 ps delay with respect to the 400 nm pump pulse to 700 ps delay. Under all delay conditions, the modulation of the response in the 3.8 nm CdSe NCs is approximately the same, indicative of a similar effective NC temperature. For ensembles, this implies that complex thermal excitations can, in principle, be used to encode the time scale at which photons are emitted; for single-photon emission sources, it may considerably reduce the time between photon emission events, speeding up the duty cycle without Auger recombination (which occurs using multiple electronic pump pulses) and with temporal control of approximately tens of picoseconds, depending upon the excitonic manifold of the sample.

Last, data in Figure 3h shows that the effect of thermal excitation when the IR beam is tuned to different wavelengths in the IR. Although the bandwidth of the femtosecond IR pump is quite broad (>1 μm at 3460 nm, see Figure S8), the absorbed power of the heat-induced secondary pulse is maximized when the center wavelength of the pump is tuned on resonance with the ligand C−H stretching vibrations. Moving to shorter or longer wavelength diminishes the intensity of the IR-induced changes. Further control experiments employed a cuvette of diluted hexanes in carbon tetrachloride as an infrared notch filter to selectively block the fraction of the pump beam resonant with the oleic acid C−H vibrations. When a hexanes filter is used, both IPEP and IR-induced PL signals are reduced substantially, despite a substantial fraction of (nonresonant) IR light still irradiating the sample. (See Figure S8.) The resonant character of this thermal excitation confirms that ligand vibrations act as antennae that facilitate NC core heating. These experiments also suggest that competing possibilities for the secondary burst of PL, in which the IR pulse resonantly excites the exciton from the dark (or other trapped) state, are unlikely, as trap distributions are typically continuous.[36,37] Additionally, several works claim that fast carrier cooling of quantum dots, which should in principle be quite slow,[38−40] is attributable to electronic interactions with ligand vibrations.[34,41−43] We note that in these experiments, there is no evidence of *p*-state emission in these NC systems at higher energies. This is true both for the initial electronic excitation and the subsequent thermal excitation. This suggests that IR excitation neither resonantly excites carriers within the electronic manifold[34,44] nor do ligand vibrations appear to couple to electronic states in such a manner to increase occupations of, for example, *p*-states, at least in the presented experiments. The observed changes are most consistent with a strictly thermal origin and the effect of temperature on the occupation of the exciton fine structure manifold of states.

In conclusion, this work demonstrates that thermal excitation of CdSe NCs, exploiting ligands as antennae, can facilitate manipulation of the instantaneous radiative rate of an ensemble. By introducing an IR excitation resonant with organic ligand vibrational energies, NCs are heated transiently above the bath temperature with a concomitant increase in the radiative rate. The burst of PL following transient heating exhibits a lifetime limited by NC thermalization (cooling) that here is roughly 2 orders of magnitude faster than the emission rate of the lowest energy excitonic state in these zinc blende CdSe NCs. Furthermore, the modulation of PL can be tuned arbitrarily in time with tens of picosecond resolution. Exploiting this effect in other systems with larger dark/bright splitting may provide opportunities to increase this difference further or, in the case of systems with bright exciton ground states,[13,16] slow radiative rates. Although presented here for ensembles, this phenomenon may prove particularly advantageous where single-photon emission is desired in a low-temperature emitter, which otherwise presents a low duty cycle and poor temporal control over photon emission.

■ ASSOCIATED CONTENT

Supporting Information

The Supporting Information is available free of charge on the ACS Publications website at DOI: 10.1021/acs.nanolett.8b04847.

Synthetic information and additional spectroscopic experiments (PDF)

■ AUTHOR INFORMATION

Corresponding Author

*E-mail: schaller@anl.gov; schaller@northwestern.edu.

ORCID

Benjamin T. Diroll: 0000-0003-3488-0213

Richard D. Schaller: 0000-0001-9696-8830

Author Contributions

The manuscript was written through contributions of both authors.

Notes

The authors declare no competing financial interest.

■ ACKNOWLEDGMENTS

This work was performed at the Center for Nanoscale Materials, a U.S. Department of Energy Office of Science User Facility, and supported by the U.S. Department of Energy, Office of Science, under Contract No. DE-AC02-06CH11357.

DOI: 10.1021/acs.nanolett.8b04847
Nano Lett. XXXX, XXX, XXX−XXX

REFERENCES

(1) Nirmal, M.; Norris, D. J.; Kuno, M.; Bawendi, M. G.; Efros, A. L.; Rosen, M. Observation of the "Dark Exciton" in CdSe Quantum Dots. *Phys. Rev. Lett.* **1995**, *75*, 3728−3731.

(2) Norris, D. J.; Bawendi, M. G. Structure in the Lowest Absorption Feature of CdSe Quantum Dots. *J. Chem. Phys.* **1995**, *103*, 5260−5268.

(3) Moreels, I.; Rainò, G.; Gomes, R.; Hens, Z.; Stöferle, T.; Mahrt, R. F. Band-Edge Exciton Fine Structure of Small, Nearly Spherical Colloidal CdSe/ZnS Quantum Dots. *ACS Nano* **2011**, *5*, 8033−8039.

(4) Norris, D. J.; Efros, A.; Rosen, M.; Bawendi, M. Size Dependence of Exciton Fine Structure in CdSe Quantum Dots. *Phys. Rev. B: Condens. Matter Mater. Phys.* **1996**, *53*, 16347−16354.

(5) Nann, T.; Riegler, J. Monodisperse CdSe Nanorods at Low Temperatures. *Chem. - Eur. J.* **2002**, *8*, 4791−4795.

(6) Naeem, A.; Masia, F.; Christodoulou, S.; Moreels, I.; Borri, P.; Langbein, W. Giant Exciton Oscillator Strength and Radiatively Limited Dephasing in Two-Dimensional Platelets. *Phys. Rev. B: Condens. Matter Mater. Phys.* **2015**, *91*, 121302.

(7) Tessier, M. D.; Biadala, L.; Bouet, C.; Ithurria, S.; Abecassis, B.; Dubertret, B. Phonon Line Emission Revealed by Self-Assembly of Colloidal Nanoplatelets. *ACS Nano* **2013**, *7*, 3332−3340.

(8) Crooker, S. A.; Barrick, T.; Hollingsworth, J. A.; Klimov, V. I. Multiple Temperature Regimes of Radiative Decay in CdSe Nanocrystal Quantum Dots: Intrinsic Limits to the Dark-Exciton Lifetime. *Appl. Phys. Lett.* **2003**, *82*, 2793−2795.

(9) Johnston-Halperin, E.; Awschalom, D. D.; Crooker, S. A.; Efros, A. L.; Rosen, M.; Peng, X.; Alivisatos, A. P. Spin Spectroscopy of Dark Excitons in CdSe Quantum Dots to 60 T. *Phys. Rev. B: Condens. Matter Mater. Phys.* **2001**, *63*, 205309.

(10) Shabaev, A.; Efros, A. L. 1D Exciton Spectroscopy of Semiconductor Nanorods. *Nano Lett.* **2004**, *4*, 1821−1825.

(11) Shabaev, A.; Rodina, A. V.; Efros, A. L. Fine Structure of the Band-Edge Excitons and Trions in CdSe/CdS Core/Shell Nanocrystals. *Phys. Rev. B: Condens. Matter Mater. Phys.* **2012**, *86*, 205311.

(12) Efros, A. L.; Rosen, M.; Kuno, M.; Nirmal, M.; Norris, D. J.; Bawendi, M. Band-Edge Exciton in Quantum Dots of Semiconductors with a Degenerate Valence Band: Dark and Bright Exciton States. *Phys. Rev. B: Condens. Matter Mater. Phys.* **1996**, *54*, 4843−4856.

(13) Sercel, P. C.; Efros, A. L. Band-Edge Exciton in CdSe and Other II−VI and III−V Compound Semiconductor Nanocrystals − Revisited. *Nano Lett.* **2018**, *18*, 4061−4068.

(14) Scholes, G. D.; Kim, J.; Wong, C. Y.; Huxter, V. M.; Nair, P. S.; Fritz, K. P.; Kumar, S. Nanocrystal Shape and the Mechanism of Exciton Spin Relaxation. *Nano Lett.* **2006**, *6*, 1765−1771.

(15) Peng, X.; Manna, L.; Yang, W.; Wickham, J.; Scher, E.; Kadavanich, A.; Alivisatos, A. Shape Control of CdSe Nanocrystals. *Nature* **2000**, *404*, 59−61.

(16) Becker, M. A.; Vaxenburg, R.; Nedelcu, G.; Sercel, P. C.; Shabaev, A.; Mehl, M. J.; Michopoulos, J. G.; Lambrakos, S. G.; Bernstein, N.; Lyons, J. L.; et al. Bright Triplet Excitons in Caesium Lead Halide Perovskites. *Nature* **2018**, *553*, 189−193.

(17) Kelestemur, Y.; Guzelturk, B.; Erdem, O.; Olutas, M.; Erdem, T.; Usanmaz, C. F.; Gungor, K.; Demir, H. V. CdSe/CdSe1-XTexCore/Crown Heteronanoplatelets: Tuning the Excitonic Properties without Changing the Thickness. *J. Phys. Chem. C* **2017**, *121*, 4650−4658.

(18) Furis, M.; Hollingsworth, J. a.; Klimov, V. I.; Crooker, S. A. Time- And Polarization-Resolved Optical Spectroscopy of Colloidal CdSe Nanocrystal Quantum Dots in High Magnetic Fields. *J. Phys. Chem. B* **2005**, *109*, 15332−15338.

(19) Bawendi, M. G.; Carroll, P. J.; Wilson, W. L.; Brus, L. E. Luminescence Properties of CdSe Quantum Crystallites: Resonance between Interior and Surface Localized States. *J. Chem. Phys.* **1992**, *96*, 946−954.

(20) Biadala, L.; Liu, F.; Tessier, M. D.; Yakovlev, D. R.; Dubertret, B.; Bayer, M. Recombination Dynamics of Band Edge Excitons in Quasi-Two-Dimensional CdSe Nanoplatelets. *Nano Lett.* **2014**, *14*, 1134−1139.

(21) Hannah, D. C.; Dunn, N. J.; Ithurria, S.; Talapin, D. V.; Chen, L. X.; Pelton, M.; Schatz, G. C.; Schaller, R. D. Observation of Size-Dependent Thermalization in CdSe Nanocrystals Using Time-Resolved Photoluminescence Spectroscopy. *Phys. Rev. Lett.* **2011**, *107*, 177403.

(22) Hannah, D. C.; Ithurria, S.; Krylova, G.; Talapin, D. V.; Schatz, G. C.; Schaller, R. D. Particle-Level Engineering of Thermal Conductivity in Matrix-Embedded Semiconductor Nanocrystals. *Nano Lett.* **2012**, *12*, 5797−5801.

(23) Huxter, V. M.; Lee, A.; Lo, S. S.; Scholes, G. D. CdSe Nanoparticle Elasticity and Surface Energy. *Nano Lett.* **2009**, *9*, 405−409.

(24) Huxter, V. M.; Scholes, G. D. Acoustic Phonon Strain Induced Mixing of the Fine Structure Levels in Colloidal CdSe Quantum Dots Observed by a Polarization Grating Technique. *J. Chem. Phys.* **2010**, *132*, 104506.

(25) Hartland, G. V. Optical Studies of Dynamics in Noble Metal Nanostructures. *Chem. Rev.* **2011**, *111*, 3858−3887.

(26) Link, S.; El-Sayed, M. A. Optical Properties and Ultrafast Dynamics of Metallic Nanocrystals. *Annu. Rev. Phys. Chem.* **2003**, *54*, 331−366.

(27) Wilson, O. M.; Hu, X.; Cahill, D. G.; Braun, P. V. Colloidal Metal Particles as Probes of Nanoscale Thermal Transport in Fluids. *Phys. Rev. B: Condens. Matter Mater. Phys.* **2002**, *66*, 224301.

(28) Hannah, D. C.; Gezelter, J. D.; Schaller, R. D.; Schatz, G. C. Reverse Non-Equilibrium Molecular Dynamics Demonstrate That Surface Passivation Controls Thermal Transport at Semiconductor-Solvent Interfaces. *ACS Nano* **2015**, *9*, 6278−6287.

(29) Diroll, B. T.; Guo, P.; Schaller, R. D. Heat Transfer at Hybrid Interfaces: Interfacial Ligand-to-Nanocrystal Heating Monitored with Infrared Pump, Electronic Probe Spectroscopy. *Nano Lett.* **2018**, *18*, 7863−7869.

(30) Sie, E. J.; McIver, J. W.; Lee, Y. H.; Fu, L.; Kong, J.; Gedik, N. Valley-Selective Optical Stark Effect in Monolayer WS2. *Nat. Mater.* **2015**, *14*, 290−294.

(31) Varshni, Y. P. Temperature Dependence of the Energy Gap in Semiconductors. *Physica* **1967**, *34*, 149−154.

(32) Kukura, P.; McCamant, D. W.; Mathies, R. A. Femtosecond Stimulated Raman Spectroscopy. *Annu. Rev. Phys. Chem.* **2007**, *58*, 461−488.

(33) Klimov, V.; Mikhailovsky, A.; McBranch, D.; Leatherdale, C.; Bawendi, M. Mechanisms for Intraband Energy Relaxation in Semiconductor Quantum Dots: The Role of Electron-Hole Interactions. *Phys. Rev. B: Condens. Matter Mater. Phys.* **2000**, *61*, R13349−R13352.

(34) Guyot-Sionnest, P.; Wehrenberg, B.; Yu, D. Intraband Relaxation in CdSe Nanocrystals and the Strong Influence of the Surface Ligands. *J. Chem. Phys.* **2005**, *123*, 074709.

(35) Wen, G. W.; Lin, J. Y.; Jiang, H. X.; Chen, Z. Quantum-Confined Stark Effects in Semiconductor Quantum Dots. *Phys. Rev. B: Condens. Matter Mater. Phys.* **1995**, *52*, 5913−5922.

(36) Anderson, P. W. Model for the Electronic Structure of Amorphous Semiconductors. *Phys. Rev. Lett.* **1975**, *34*, 953−955.

(37) Street, R. A.; Mott, N. F. States in the Gap in Glassy Semiconductors. *Phys. Rev. Lett.* **1975**, *35*, 1293−1296.

(38) Benisty, H.; Sotomayor-Torrès, C. M.; Weisbuch, C. Intrinsic Mechanism for the Poor Luminescence Properties of Quantum-Box Systems. *Phys. Rev. B: Condens. Matter Mater. Phys.* **1991**, *44*, 10945−10948.

(39) Benisty, H. Reduced Electron-Phonon Relaxation Rates in Quantum-Box Systems: Theoretical Analysis. *Phys. Rev. B: Condens. Matter Mater. Phys.* **1995**, *51*, 13281−13293.

(40) Bockelmann, U.; Bastard, G. Phonon Scattering and Energy Relaxation in Two-, One-, and Zero-Dimensional Electron Gases. *Phys. Rev. B: Condens. Matter Mater. Phys.* **1990**, *42*, 8947−8951.

(41) Peterson, M. D.; Cass, L. C.; Harris, R. D.; Edme, K.; Sung, K.; Weiss, E. a. The Role of Ligands in Determining the Exciton Relaxation Dynamics in Semiconductor Quantum Dots. *Annu. Rev. Phys. Chem.* **2014**, *65*, 317−339.

DOI: 10.1021/acs.nanolett.8b04847
Nano Lett. XXXX, XXX, XXX−XXX

(42) Bozyigit, D.; Yazdani, N.; Yarema, M.; Yarema, O.; Lin, W. M. M.; Volk, S.; Vuttivorakulchai, K.; Luisier, M.; Juranyi, F.; Wood, V. Soft Surfaces of Nanomaterials Enable Strong Phonon Interactions. *Nature* **2016**, *531*, 618−622.
(43) Aharoni, A.; Oron, D.; Banin, U.; Rabani, E.; Jortner, J. Long-Range Electronic-to-Vibrational Energy Transfer from Nanocrystals to Their Surrounding Matrix Environment. *Phys. Rev. Lett.* **2008**, *100*, 057404.
(44) Wehrenberg, B. L.; Wang, C.; Guyot-Sionnest, P. Interband and Intraband Optical Studies of PbSe Colloidal Quantum Dots. *J. Phys. Chem. B* **2002**, *106*, 10634−10640.

DOI: 10.1021/acs.nanolett.8b04847
Nano Lett. XXXX, XXX, XXX−XXX